Water-oxidation mechanism of cobalt phosphate co-catalyst in artificial photosynthesis: a theoretical study

Takao Tsuneda[a,b*] and Seiichiro L. Ten-no[a]

[a] *Graduate School of Science, Technology, and Innovation, Kobe University, Kobe 657-8501, Japan and*

[b] *Department of Chemistry, Faculty of Science, Hokkaido University, Sapporo 060-0810, Japan*

Abstract

The initial water-oxidation reaction mechanism of the hydrated cobalt phosphate (CoPi) co-catalyst, which is consistent with conventional experimental findings, is investigated for the O–O bond and OOH formations in this study. Theoretical calculations of hydrated CoPi cluster models, which are validated by vibrational spectrum calculations, elucidate the roles of phosphate as a resource of oxygen and deliverer of protons, both of which result in the spontaneous formation of an O–O bond after the release of two electrons and two protons. The calculations also show that the OOH formation proceeds subsequently depending on the spin electronic states of the hydrated CoPi surface, and the O_2 formation then spontaneously progresses after the release of two electrons and two protons. By theoretically tracing these processes, the initial water-oxidation reaction mechanism of the hydrated CoPi co-catalyst is proposed.

I. INTRODUCTION

Cobalt phosphate (CoPi) is one of the most popular water-oxidation co-catalysts in artificial photosynthesis.[1] Artificial photosynthesis has attracted attention as a sustainable method for generating hydrogen from water and solar energy.[2,3] The use of CoPi is sustainable because it is synthesized from cobalt solution and phosphate (HPO_4^{2-}), which are both earth-abundant materials, and it is active even in neutral water under ambient conditions. In artificial photosynthesis, CoPi is used to promote the efficiency of photo-induced water-oxidation catalysts such as $BiVO_4$ and α-Fe_2O_3 (hematite), which are usually n-type semiconductors with visible-light band gaps. CoPi provides a 15-fold enhancement in the oxygen evolution (water oxidation) rate of $BiVO_4$ in neutral water.[4] According to the pH dependence of the catalytic activity, Surendranath et al. suggested that CoPi incorporates a mechanism of the reversible release of electrons and protons in water oxidation in the range of pH 4–12.[5] Kanan and Nocera indicated that the hydrogen phosphate ion is used as a proton acceptor in water oxidation.[1] However, it has thus far not been revealed how the water-oxidation reaction proceeds in the case of CoPi, especially in terms of the rate-determination process and the detailed contributions of the phosphate species in the reaction.

The water-oxidation reaction mechanism of CoPi has been investigated in many experimental studies.[4–9] Lutterman et al. proposed that phosphate repairs the cobalt-oxide surface, which undergoes degradation after the application of an electric potential, by facilitating the oxidation of Co(II) to Co(III) centers, while the Co(III) centers are substantially too inactive to participate in this reaction.[6] Based on Tafel slope analyses, Surendranath et al. suggested a turnover-limiting water-oxidation mechanism, in which a rapid one-electron and one-proton equilibrium called "proton-coupled electron transfer equilibrium" is maintained between Co(III)OH and Co(IV)O by the medium of the phosphate species, which acts as a proton acceptor.[5] McAlpin et al. provided electron paramagnetic resonance (EPR) evidence for the transition from Co(II) to Co(IV) centers with negligible signals of Co(III) centers during the water oxidation, and assumed that the negligible EPR signals come from the silent low-spin Co(III) centers.[7] We, however, interpret that the negligible signals may partly come from the relatively fast electron-pair release producing Co(IV) centers from Co(II), because Lutterman et al. indicate that the Co(III) centers are too inactive to par-

ticipate in this reaction, as mentioned above.[6] Using the time-resolved Fourier-transform infrared (FTIR) spectroscopy of cobalt-oxide nanoparticles with no phosphate. Zhang et al. observed the reaction intermediates and proposed that the water-oxidation reaction of a cobalt-oxide surface proceeds according to the following process:[9]

1. Cobalt-oxide hydroxylation takes place.
2. Co(III)-OH is then converted into Co(IV)=O.
3. Nucleophilic H_2O addition to one oxo site occurs.
4. An O–O bond is formed to create an OOH group.
5. O_2 is finally produced by the proton transfer from the OOH group to a neighboring Co(IV)=O site.

They also suggested that the water oxidation rate depends on the presence/absence of neighboring Co(IV)=O sites. In terms of the contribution of the phosphate species, Barroso et al. observed a significant retardation of the electron dynamics decay in the transient absorption spectroscopy of α-Fe_2O_3/CoPi and explained that the activity enhancement of CoPi is partially owing to the reduced charge recombination losses due to the formation of a Schottky-type heterojunction.[8] Jeon et al. also found that the incorporation of phosphate into cobalt-oxide surface on $BiVO_4$ is kinetically slower than water oxidation and suggested that CoPi makes electrons more mobile and increases conductivity.[4] Although many experimental studies have been conducted on the water oxidation of CoPi, as mentioned above, the reaction mechanism involved is still unknown in terms of various aspects. In particular, it is unclear how the presence of phosphate contributes to the reaction mechanism, although it has been explained that the phosphate acts as a proton acceptor in the water oxidation.

Thus far, there have been few theoretical studies on the water-oxidation reaction of CoPi.[10–12] Using a periodic boundary condition (PBC) calculation, Chen et al. explored the potential-dependence of the hydrated cobalt-oxide surface structures and free energy diagrams.[10] They, consequently, suggested that the rate-determining process is the OH deprotonation, which is active only on the positively-charged surface. Pham et al. also used a PBC calculation to investigate the hydrated cobalt-oxide surface.[11] As a result, they similarly concluded that this reaction occurs by the OH deprotonation, and suggested a water

oxidation reaction mechanism, which is different from the above experiment-based mechanism in the number of released protons and electrons: five protons and five electrons as a whole. Wang and van Voorhis studied the catalytic water-oxidation mechanism of CoPi using a cubane model of cobalt-oxide surface, while neglecting phosphate, wherein the surface is initially hydroxylated.[12] This model is based on the experimental evidence that the water oxidation slowly proceeds even without phosphate, and the cubane model is suggested as a cobalt-oxide structure in an X-ray absorption spectroscopy study.[13] As a result, they found that the O–O bond formation proceeds with a very low reaction barrier (approximately 4 kcal/mol) and suggested that this low barrier is caused by the oxidation of Co(III)-OH to Co(IV)=O, as explained experimentally.[9] However, this study presents several controversial points while discussing the water oxidation reaction of CoPi: the initial hydroxylation mechanism of the CoPi surface remains to be determined, phosphate is neglected irrespective of its significant contribution to the reaction, the corner-edged cubane is investigated in an X-ray absorption spectrum study[14] that proposes a corner-sharing molecular cobaltate cluster (MCC) as alternated, and the hydrogen-bond networks around the model are disregarded despite the donation/acceptance of protons in the reaction. All these points should be considered for theoretically simulating the actual water-oxidation reaction of the hydrated CoPi surface.

In this study, we theoretically investigate the initial water-oxidation reaction mechanism of a hydrated CoPi surface, which is consistent with the above-mentioned experimental findings, using the cluster models of the cobalt-oxide surface, which adsorbs hydrated phosphate ($HPO_4{}^{2-}$) and water molecules. Both the singlet and doublet electronic states of the cobalt-oxide surface cluster models are examined to take into consideration the paramagnetic effect of the cobalt-oxide surface.[7] In the calculations, we apply a long-range correction (LC)[15,16] for the density functional theory,[17,18] which can quantitatively provide occupied and unoccupied valence orbital energies[19,20] and has been confirmed to correctly reproduce various charge-transfer-driven electrochemical reactions.[21–25] Based on the calculated results, we reveal the driving force of the water-oxidation reaction and the roles of phosphate.

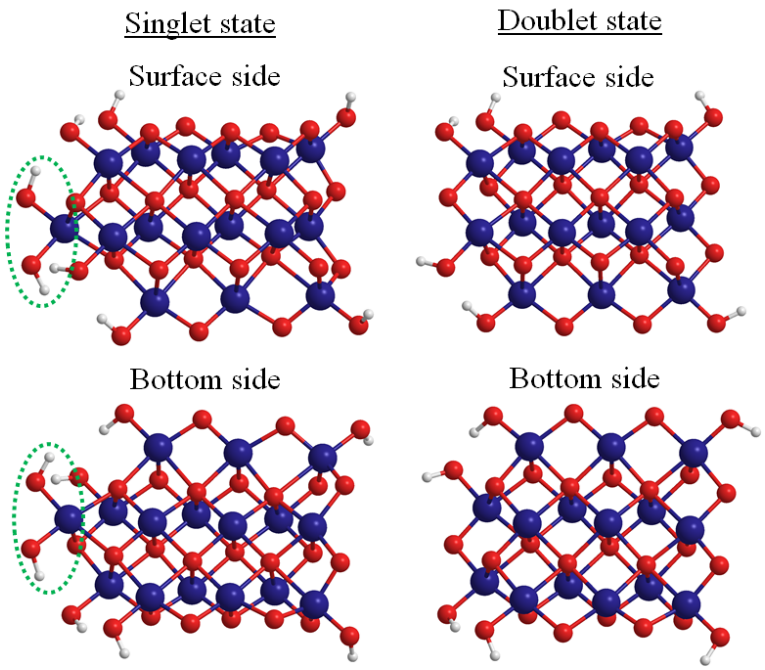

FIG. 1: Calculated cluster models of a cobalt-oxide surface for the singlet and doublet electronic states from the surface and bottom sides. The difference between the models of the singlet and doublet states, which is the $Co(OH)_2$ fragment, is indicated by green dotted circles.

II. COMPUTATIONAL DETAILS

The water-oxidation reaction of CoPi is investigated by performing calculations using a hydrated CoPi model, wherein hydrated phosphate adsorbs the cobalt-oxide surface cluster. In the case of the cobalt-oxide surface, the experimentally supported MCC model of a double-layer cobalt-oxide cluster is adopted for the singlet and doublet electronic structures, based on the experimental findings of the cobalt-oxide surface[7,8,14] (Fig. 1). Note that since this MCC model shares a common crystal system with the edge-sharing cubane model, which is observed in an X-ray pair distribution function analysis,[26] this MCC model gives the same structure as that of the edge-sharing cubane model after performing the full geometry optimization. The size of the cobalt oxide cluster model is determined to be sufficient for the calculations of this reaction including two adsorption sites of phosphate, four neighboring water-adsorption sites for forming the O–O bond, and the underlayer of the surface for releasing and accepting electrons. In the cluster model, the endpoint oxygen atoms of the

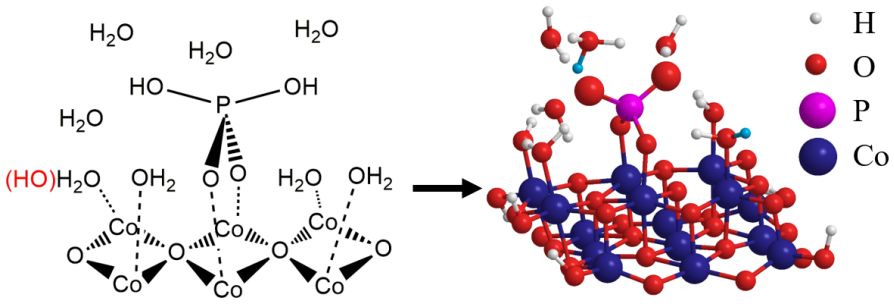

FIG. 2: Reactant structures of hydrated CoPi surface cluster model: the left-hand-side figure presents a schematic view of the calculated surface cluster model, and the right-hand-side figure presents the optimum geometry of the cluster model for the singlet-state cobalt-oxide surface model. As shown in the surface structure model, one hydrogen is removed from one adsorbing water molecule for the singlet-state surface cluster model, wherein the water molecules with removed hydrogen are indicated by (OH)" in red beside the corresponding water molecules. From the right-hand-side reactant structure, two hydrogen atoms, which are highlighted in light blue, are initially removed.

model on the bottom sides are terminated by the bonding of hydrogen. Note that this cluster model is very different from the normal spinel structure of the standard Co_3O_4 crystal, which includes both tetrahedral Co(II) and octahedral Co(III) centers and requires broken symmetry calculations due to its antiferromagnetic nature. The reactant structure of the CoPi surface cluster model incorporates the adsorption of phosphate ($H_2PO_4^-$), which is explicitly hydrated by four water molecules and coordinates two oxygen atoms to the Co sites with four water molecules (or four water molecules and one OH group) occupying the remaining Co sites of the surface (Fig. 2). As shown in Fig. 2, water molecules occupy all the adsorption sites of the surface except for the two adsorption sites of phosphate, while other four water molecules are explicitly included to model the hydrogen bond network around the phosphate with a minimum number of water molecules.

Geometry optimizations are performed using the Kohn–Sham density functional theory (DFT) calculations[17,27] with the LC[15,16] for the Becke 1988 exchange[28] plus Lee-Yang-Parr correlation[29] functional (the only parameter $\mu = 0.33$[30]). The LC is employed to include long-range exchange interactions, which are required to quantitatively investigate chemical reactions,[31] because generalized-gradient-approximation exchange functionals, which are frequently used in solid-state calculations using PBCs, have delocalization errors[32] and cover

long-range interactions only up to 5Å on surface.[33,34] Note that cluster models have both advantages and disadvantages against PBC slab models in reaction calculations: Though PBC slab models reproduce correct electronic conductions in solid surfaces due to near-zero band gaps of solid states, cluster models usually have well-balanced electron correlations that are required to investigate chemical reactions due to the use of sophisticated functionals like LC functionals. The cc-pVDZ basis set[35,36] is used for the H, O, and P atoms, and the LANL2DZ effective core potential basis set[37] is employed for the Co atom. For the solvent effect, the polarizable continuum model[38] of water is included. It should be noted that several initial structures are examined to determine the optimum geometries. In this study, various spin multiplicities are examined for the cluster models to make clear the dependence of the water oxidation reaction on the spin states of CoPi surface. The singlet and triplet electronic states of the hydrated cluster models are first explored for both the singlet- and doublet-state cobalt-oxide surfaces. This is because the study on the degradation of CoPi shows that the Co(III) centers, which are produced after the release of one electron, are too inactive to participate in the reaction[6]. We interpret that this result implies that electrons are released in steps of two to proceed the catalytic reaction. Following this interpretation, the doublet and quartet electronic states for the doublet-state cobalt-oxide surface are also examined as other paramagnetic states. The total charge of the model is maintained at zero during the reaction process, while assuming that the protons are coincidentally generated and removed with electrons. That is, hydrogen atoms are removed from the hydrated water molecules around phosphate in the reaction process of reactant → Min1 and Min2 → Min3, as explained subsequently. The potential energy calculations are performed by optimizing the geometry of the whole system with fixing only the target bond distance for each reaction. Note that the optimum geometries of the reactants are obtained even for the barrierless structures without dropping into the products, because the potential energy curves are usually plateau near the reactants. Several initial structures are examined in all optimization calculations. The energies are evaluated for the case of zero temperature. The Gaussian 09 suite of programs[39] is used to perform all the geometry optimizations. All of the optimized structures are checked to ensure that they yield positive, real frequencies.

For examining the validity of the cluster model, the vibrational spectrum of the hydrated CoPi cluster model using the doublet-spin cobalt-oxide surface in the singlet state is first compared to the experimental FTIR spectrum of CoPi surface[40] in Fig. 3 (see Fig. S1 of

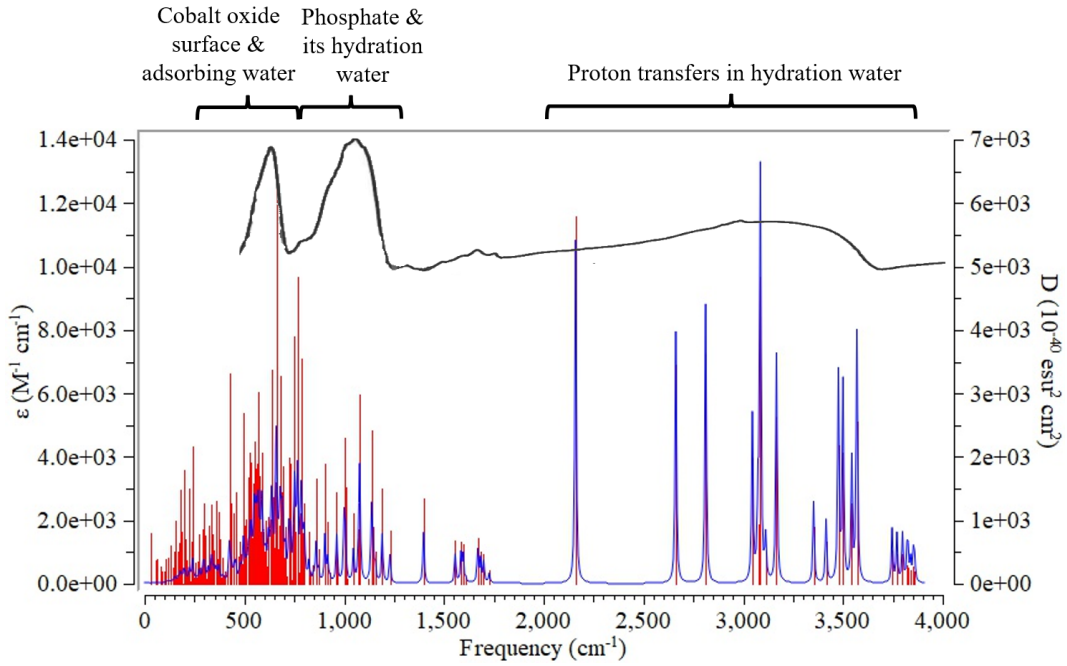

FIG. 3: Calculated vibrational spectrum of hydrated CoPi cluster model for the optimized reactant structure using the doublet-state cobalt-oxide surface in the singlet state. The curve at the top is the experimental FTIR spectrum of CoPi surface, which is excerpted from Ref.[40] for comparison. The main vibrational spectral band assignment is also shown.

Supporting Information for the vibrational spectrum of the cluster model using the singlet-spin cobalt-oxide surface in the singlet state). The figure clearly shows that the cluster model correctly provides the characteristic IR peaks in the region of 400 through 1250 cm^{-1}. Note that the IR peaks in the range of 800 through 1250 cm^{-1} disappear for the phosphate-less cobalt oxide surface in the experimental IR spectrum.[40] This experimental finding is supported by the assignment of the calculated peaks, in which the peaks in the region from 800 to 1250 cm^{-1} correspond to the vibrations of the phosphate and its hydration water molecules. The calculated vibrational spectrum of the cluster model using the singlet-state cobalt-oxide surface in the same singlet state is also illustrated in Fig. S1. The figure shows that it gives slightly-different vibrational spectral peaks from that of the doublet-state surface especially in the region of 400 through 1250 cm^{-1}, indicating the high sensitivity of the vibrational spectra to the calculation model. Since the vibrational spectrum of the doublet-state cobalt-oxide surface appears to be closer to the experimental IR spectrum than that of the singlet-state surface, it suggests that CoPi surface has the doublet-state cobalt-

oxide surface in, at least, the unbiased condition. This is consistent with the experimentally-observed paramagnetism of CoPi surface.[7] Therefore, along with the consistence with the experimental findings, this vibrational spectrum also establishes the validity of this CoPi cluster model, vindicating the reproducibility of the water oxidation reaction including the reaction paths through transition states.

III. RESULTS AND DISCUSSIONS

A. Water-oxidation reaction of hydrated CoPi surface on doublet-state surface

Let us first focus on the water-oxidation reaction process for the cluster model of the hydrated CoPi surface in the singlet and triplet electronic states on the doublet-state cobalt-oxide surface.

As shown in the reactant CoPi structure presented on the right side of Fig. 2, the phosphate on the cobalt-oxide surface coordinates to a hydrating water molecule in the optimized reactant structures of the hydrated CoPi surface. It should be noted that phosphorus compounds often form a fifth bond with oxygen, thus violating the octet rule, e.g., triphenylphosphine oxide ($O{=}P(Ph)_3$) forms a fifth bond with hydrogen peroxide.[41] The optimum geometry also demonstrates that phosphate possesses high proton conductivity, because it forms hydrogen bond networks of the non-adsorbed oxygen atoms with adsorbing and hydrated water molecules. This implies that phosphate plays two roles: bond formation with the hydrating water molecules and hydrogen-bond network formation with the surface water molecules.

In the first reaction process (Reactant $\rightarrow$ Min1), two hydrogen atoms, i.e., two electrons and two protons, which are shown in light blue in the right-hand-side of Fig. 2, are released from the hydrated water molecules around the phosphate of the reactant CoPi structure. This electron-pair release and the subsequent release of two protons are based on the inactivity after the release of one electron proposed in the degradation study of CoPi surface[6] and the proton-coupled electron transfer equilibrium.[5] In Fig. 4, the optimum structures of the hydrated CoPi model obtained after releasing two hydrogen atoms are indicated by "Min1" for the (a) singlet and (b) triplet states of the calculation model. The optimum geometries of Min1 show that the O–O bonds are formed naturally after the two hydrogen

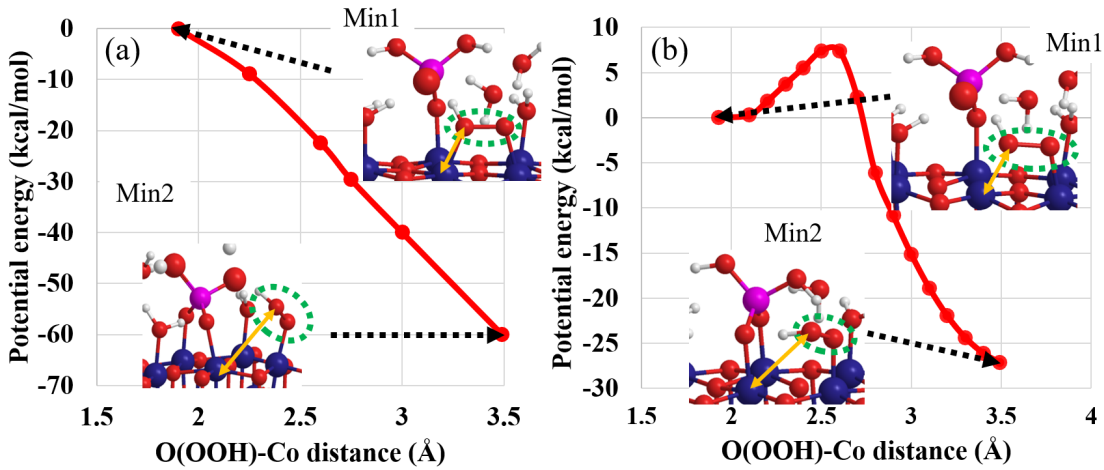

FIG. 4: Potential energy curves of the hydrated CoPi cluster model using the doublet-state cobalt-oxide surface cluster model in the (a) singlet and (b) triplet electronic states for the extension of the distance between an O atom of the OOH group and the Co atom of its adsorption site. The potential energy is set as zero for the optimum hydrated CoPi structure before extending the O–Co distance. The optimum structures of the CoPi model before and after extending the O–Co distances are indicated by Min1 and Min2, respectively. In these optimum structures, the extended O–Co distances are indicated by orange arrows, and the formed O–O bonds are indicated by green dotted circles.

atoms are released in the case of both the singlet and triplet states. This spontaneous O–O bond formation is attributed to the use of phosphate, because previous theoretical studies have suggested that the O–O bond formation is a key process of this reaction for cobalt-oxide surface.[10–12] It should be noted that the hydrogen atoms are initially released from the hydrated water molecules around the phosphate in both cases. This indicates that, by releasing the hydrogen atoms from the two adsorbing H_2O molecules through the hydrogen bond network around the phosphate, the first reaction step spontaneously proceeds to release the hydrogen atom from the Co–OH site neighboring an adsorption site of the phosphate, as experimentally suggested.[9]

After the spontaneous O–O bond formation (Min1), an OOH group is formed by desorbing one O atom from an adsorption site: Min1 → Min2. This is based on the experimental time-resolved FTIR spectroscopy study that showed that the OOH group is formed after the O–O bond is formed.[9] The O–Co distance between an O atom of the formed OOH group and the

Co atom of the adsorption site is extended to investigate this process. Figure 4 displays the potential energy curves in terms of the extension of the O–Co distance for the singlet and triplet states of the hydrated CoPi surface. The figure shows that the potential energy curve of the doublet-state surface monotonically decreases for the singlet state, while it has a low reaction barrier of approximately 8 kcal/mol for the triplet state. The structures of "Min2" in Fig. 4 indicate the optimized structures of the hydrated CoPi model after the dissociation of the O–Co bond. As shown in the figures, the singlet and triplet states provide similar optimum geometries for both Min1 and Min2. The geometries demonstrate that one oxygen atom of the phosphate simultaneously occupies the vacant adsorption site after the O–Co bond dissociation.

For investigating the dependence of the OOH-formation reaction on the spin state of the hydrated CoPi surface in further detail, we also examined the doublet and quartet states for the doublet-state cobalt-oxide surface. Figure 5 illustrates the potential energy curves in terms of the extension of the O–Co distance for the doublet- and quartet states of the hydrated CoPi surface. This corresponds to the aforementioned third possibility for the magnetism of the hydrated CoPi surface. It should be noted that the quartet state is calculated to be slightly more stable than the doublet state by 14.6 and 3.9 kcal/mol for Min1 and Min2, respectively. As shown in the figure, considerable reaction barriers are formed for both the doublet and quartet states: approximately 20 and 10 kcal/mol, respectively. This suggests that very small OOH formation rates may be given for the doublet- and quartet-state hydrated CoPi surface of the doublet-state cobalt-oxide surface.

It should be noted that the experimental EPR study shows that the water-oxidation reaction proceeds not in the diamagnetic state (singlet state) but in the paramagnetic state.[7] This finding indicates the following three possibilities for the magnetism of the hydrated CoPi surface in this reaction:

1. The entire system of the hydrated CoPi surface is paramagnetic.

2. Only the cobalt-oxide surface is paramagnetic.

3. The hydrated CoPi and cobalt-oxide surfaces are both paramagnetic.

In this section, we have explored the water-oxidation reaction on the doublet-state cobalt-oxide surface and found that this reaction spontaneously proceeds for the triplet state of

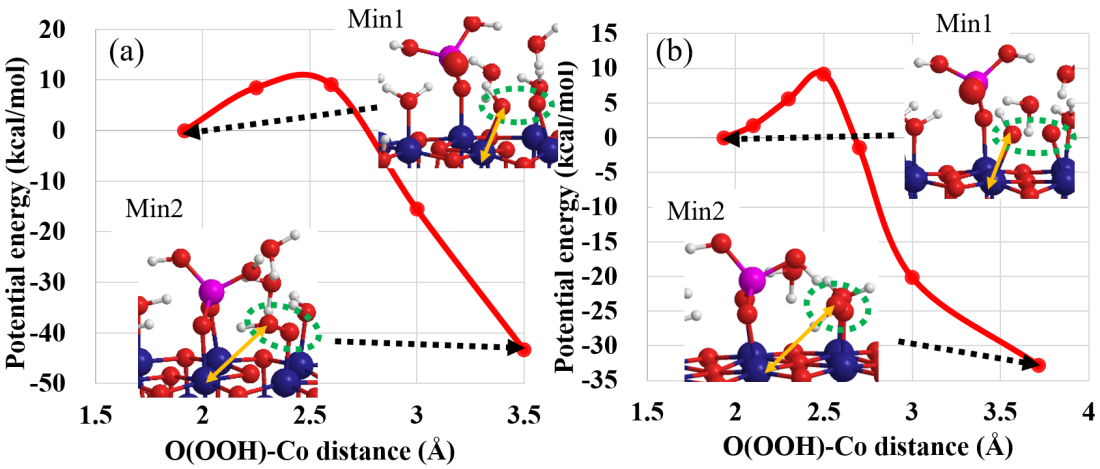

FIG. 5: Potential energy curves of the hydrated CoPi cluster model using the doublet-state cobalt-oxide surface cluster model in the (a) doublet and (b) quartet electronic states for the extension of the distance between an O atom of the OOH group and the Co atom of its adsorption site. The potential energy is set as zero for the optimum hydrated CoPi structure before extending the O–Co distance. The optimum structures of the CoPi model before and after extending the O–Co distances are also indicated by Min1 and Min2, respectively. In these optimum structures, the extended O–Co distances are indicated by orange arrows, and the formed O–O bonds are indicated by green dotted circles.

the hydrated CoPi surface. Therefore, the calculated result is consistent with all these possibilities.

B. Water-oxidation reaction of hydrated CoPi surface on singlet-state surface

Similar to the reaction on the doublet-state cobalt-oxide surface, the water-oxidation reaction process of the hydrated CoPi surface is explored for the singlet-state cobalt-oxide surface in the singlet and triplet electronic states. The phosphate coordinates a hydrating water molecule in the reactant of the hydrated CoPi surface with the singlet-state surface as well as that of the doublet-state surface (see Fig. S2 in Supporting Information).

For the first reaction process (Reactant → Min1), the optimized structure of the hydrated CoPi surface before and after releasing two hydrogen atoms is presented in the right side of Fig. 6. The figures show that, in a manner similar to the reaction on the doublet-state cobalt-oxide surface, the O–O bond is formed naturally after the hydrogen atoms are

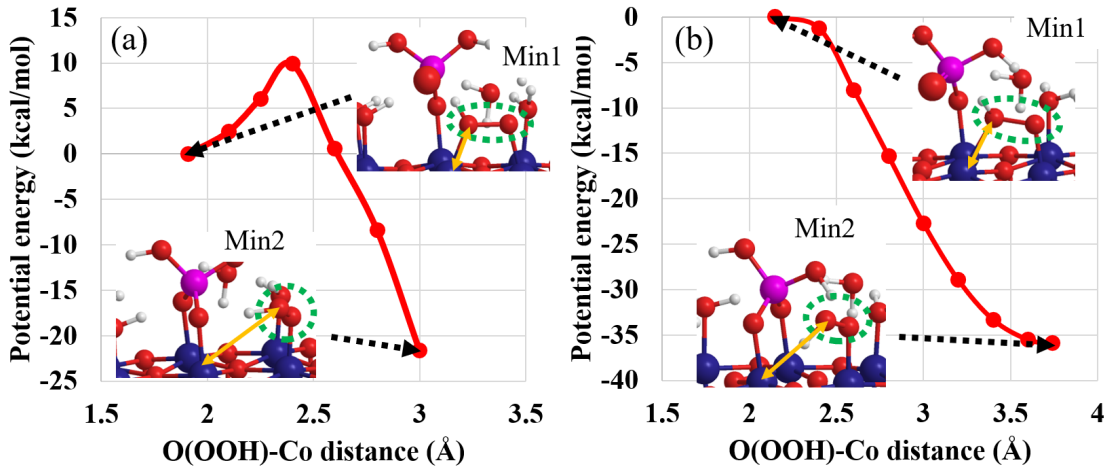

FIG. 6: Potential energy curves of hydrated CoPi cluster model using the singlet-state cobalt-oxide surface cluster model in the singlet and triplet electronic states for the extension of the distance between an O atom of the OOH group and the Co atom of its adsorption site. The potential energy is set as zero for the optimum hydrated CoPi structure before extending the O–Co distance. The optimum structures of the CoPi model before and after extending the O–Co distances are also indicated by Min1 and Min2, respectively. In these optimum structures, the extended O–Co distances are indicated by orange arrows, and the formed O–O bonds are indicated by green dotted circles.

removed for both the (a) singlet and (b) triplet states on the doublet-state surface. This shows that the O–O bond is formed on the CoPi surface irrespective of the electronic states of the cobalt-oxide surface owing to the release of two protons and two electrons from the hydrogen bond network around the phosphate.

However, the calculated results show that the second reaction process (Min1 → Min2) depends significantly on the spin states of the cobalt-oxide surface. Figure 6 illustrates the potential energy curves of the hydrated CoPi surface model in the (a) singlet and (b) triplet states for the extension of the O–Co distance. As shown in the figure, in contrast to the case of the doublet-state cobalt-oxide surface, the potential energy of the triplet state monotonically decreases with no reaction barrier for the desorbing of one side of the formed OOH group, while that of the singlet state has a low barrier of approximately 10 kcal/mol. This result indicates that, on the singlet-state surface, the OOH group formation[9] proceeds spontaneously for the triplet state. This may be supported by the experimental

study on the degradation of CoPi[6] indicating that the low-spin Co(III) centers, which may correspond to the singlet-state hydrated CoPi with the single-state cobalt oxide surface due to the negligible EPR signals,[7] are substantially too inactive to participate in the catalytic reaction. This indicates that the spin state of the cobalt-oxide surface significantly affects the reactivity irrespective of the spin states of the hydrated CoPi surface. It should be noted that the triplet state of the hydrated CoPi surface model is much more stable than its singlet state: the former is 79.3 kcal/mol and 77.2 kcal/mol more stable than the latter for Min1 and Min2, respectively. These results indicate that, on the singlet-state cobalt-oxide surface, the OOH formation proceeds in the region of the triplet state of the hydrated CoPi surface. It should also be noted that the spin state of the cobalt-oxide surface significantly affects the OOH formation energies: the singlet state of the hydrated CoPi surface provides 22 kcal/mol and 60 kcal/mol and the triplet state provides 36 kcal/mol and 27 kcal/mol for the singlet- and doublet-state cobalt-oxide surfaces, respectively. It is, therefore, suggested that the difference in the spin states of the surface, which may be due to the defects and crystal structures of the surfaces, significantly affects the water oxidation reactivity of CoPi in the process of the OOH group formation.

Based on the above results, the entire water-oxidation reaction of the hydrated CoPi surface on the doublet-spin cobalt-oxide surface is clarified. Figure 7 illustrates the entire reaction mechanism for the singlet-state hydrated CoPi with the doublet-state cobalt-oxide surface After the OOH formation (Min2), two hydrogen atoms, i.e., two electrons and two protons, are released from the hydrated water molecules around the phosphate. The optimized structure obtained after the removal of two hydrogen atoms (Min3) in the figure indicates that an adsorbing O_2 molecule is spontaneously formed by the proton transfer through the hydrogen bond network. This indicates that O_2 is spontaneously produced after the OOH formation. In the subsequent process, it is expected that one water molecule then comes close to the O_2 molecule (Min4) and is substituted for the adsorbing O_2 molecule (Product). The water-oxidation reaction finally comes full circle with the acceptance of one water molecule. It should be noted that similar mechanisms are obtained for other combinations of the singlet- and triplet-state hydrated CoPi surface with the singlet- and doublet-state cobalt-oxide surfaces (see Figs. S3 through S5 in Supporting Information). It is, therefore, concluded that the water-oxidation reaction of the hydrated CoPi surface proceeds based on this mechanism, wherein the O–O bond and O_2 formations occur spon-

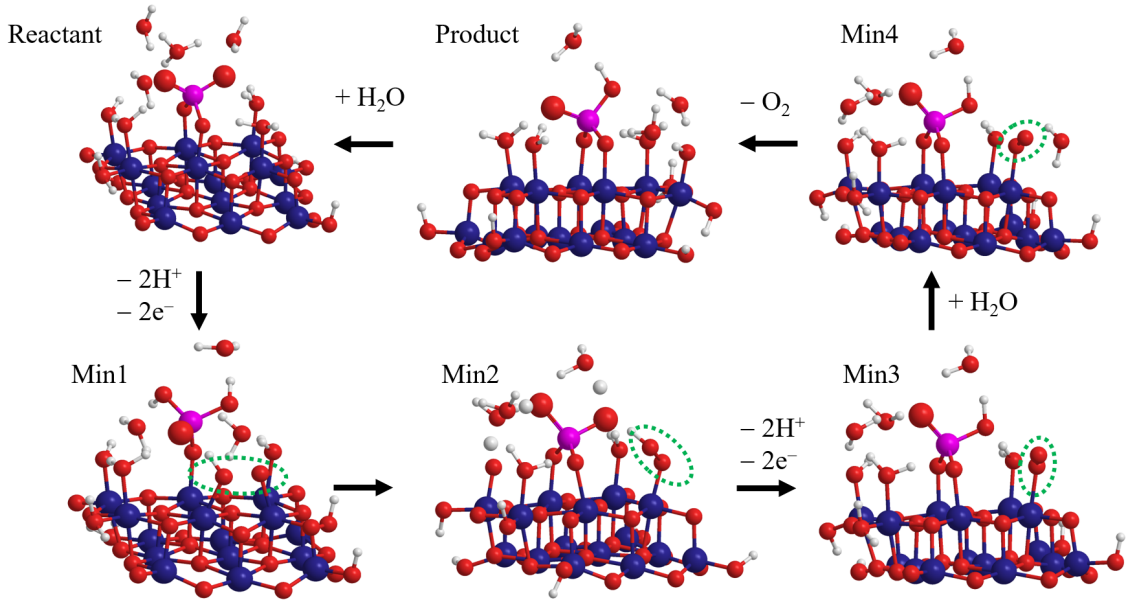

FIG. 7: Water-oxidation reaction mechanism of hydrated CoPi surface in the singlet state for the doublet-state cobalt-oxide surface. The formed O–O bonds are indicated by green circles.

taneously by the release of two electrons and two protons, and the OOH formation plays a major role in this.

Finally, let us consider the electron release that proceeds with the proton release in the processes from the reactant to Min1 and from Min2 to Min3. Figure 8 presents the molecular orbitals of the hydrated CoPi surface, from which two electrons are supposed to be released. As shown in the figure, the HOMO is mainly distributed in the cobalt-oxide surface for the reactant, while the HOMO in the singlet state and the SOMO in the triplet state are mainly found in the OOH group for Min2. This indicates that, although electrons are released from the cobalt-oxide surface in the initial reaction process, they are donated from the OOH group after its formation to facilitate the proton release of the OOH group. It should be noted that this result is consistent with the successive reaction processes that occur after the release of electrons in the water-oxidation reaction mechanism (Fig. 7).

IV. CONCLUSIONS

In this study, we investigated the water-oxidation reaction mechanism of a hydrated CoPi surface for the O–O bond and OOH formations while taking into consideration the conven-

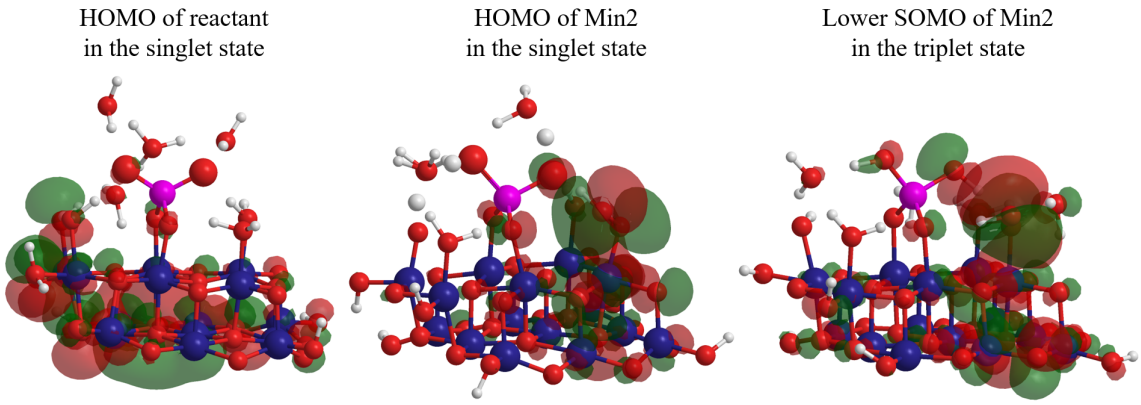

FIG. 8: Highest occupied molecular orbital (HOMO) image of the reactant in the singlet state and the HOMO and lower singly occupied molecular orbital (SOMO) images of Min2 in the singlet and triplet states, respectively, of the hydrated CoPi surface model, from which two electrons are released in the processes from reactant to Min1 and from Min2 to Min3 in the water-oxidation reaction mechanism (Fig. 7).

tional experimental findings in terms of the MCC model, paramagnetism, and electron-pair release during the reaction. Consequently, we succeeded in proposing the roles of the phosphate, the spin-dependence of the OOH formation, and the initial mechanism of the water-oxidation reaction.

The calculations were performed using two cluster models, i.e., doublet- and singlet-state models, while focusing on the reaction processes toward the formation of the OOH group for various combinations of the spin electronic states of the hydrated CoPi and the cobalt-oxide surfaces. For the cluster models, the calculated vibrational spectra of the reactant structures were first compared to the experimental FTIR spectrum of CoPi surface[40] in order to test the cluster models. Consequently, we found that the FTIR spectra are accurately reproduced by the vibrational spectra, establishing the validity of the cluster models. We, then, explored the initial reaction process after the release of two electrons and two protons in the presence of phosphate. As a result, we found that the O–O bond is spontaneously formed independent of the spin electronic states in the process that the phosphate strongly coordinates the oxygen of a hydrated water molecule, and it then releases an oxygen that adsorbs the cobalt-oxide surface to form an O–O bond with the oxygen of a neighboring hydroxyl group. This indicates that releasing one oxygen atom to form the O–O bond is the main role of phosphate in this reaction. The successive OOH formations were found to be

significantly dependent on the spin electronic states of the hydrated CoPi and the cobalt-oxide surfaces: the OOH formation spontaneously proceeds for the triplet-state hydrated CoPi surface with the singlet-state cobalt-oxide surface and the singlet-state hydrated CoPi surface with the doublet-state cobalt-oxide surface, while it has considerable reaction barriers for other combinations of the spin states. In the case of the process following the OOH formation, it was found that the release of two electrons and two protons spontaneously forms O_2, which then desorbs via a displacement with a hydrated water molecule in the presence of phosphate. This reaction mechanism was supported by illustrating the distributions of the released electrons in the hydrated CoPi surface.

In summary, we succeeded in proposing the initial water-oxidation reaction mechanism of the hydrated CoPi surface. Figure 9 presents a presumed schematic of the water-oxidation reaction. Experimentally, this reaction mechanism can be verified by, e.g., synthesizing an isotopically-substituted CoPi, in which the oxygen atoms of only phosphate are substituted by oxygen isotopic atoms. That is, the reaction mechanism is confirmed by checking that this isotopically-substituted CoPi generates oxygen molecules containing the isotopic oxygen atoms after the catalytic reaction. We hope that the revealed initial water-oxidation reaction mechanism will contribute to the future development of artificial photosynthetic systems.

ACKNOWLEDGMENTS

This study was supported by the Japanese Ministry of Education, Culture, Sports, Science and Technology (MEXT) (Grants: 17H01188 and JP18H03900). This study was also partly supported by MEXT as "Priority Issue on Post-K computer" (Development of new fundamental technologies for high-efficiency energy creation, conversion/storage and use).

SUPPORTING INFORMATION

The calculated vibrational spectrum of the hydrated CoPi cluster model for the optimized reactant structure using the singlet-state cobalt-oxide surface in the singlet state is illustrated in Fig. S1. The images of the optimum geometries of the reactant structure of the hydrated CoPi surface cluster model are presented for the singlet- and doublet-state cobalt-oxide surfaces in Fig. S2. The water-oxidation reaction mechanisms of the hydrated CoPi surface

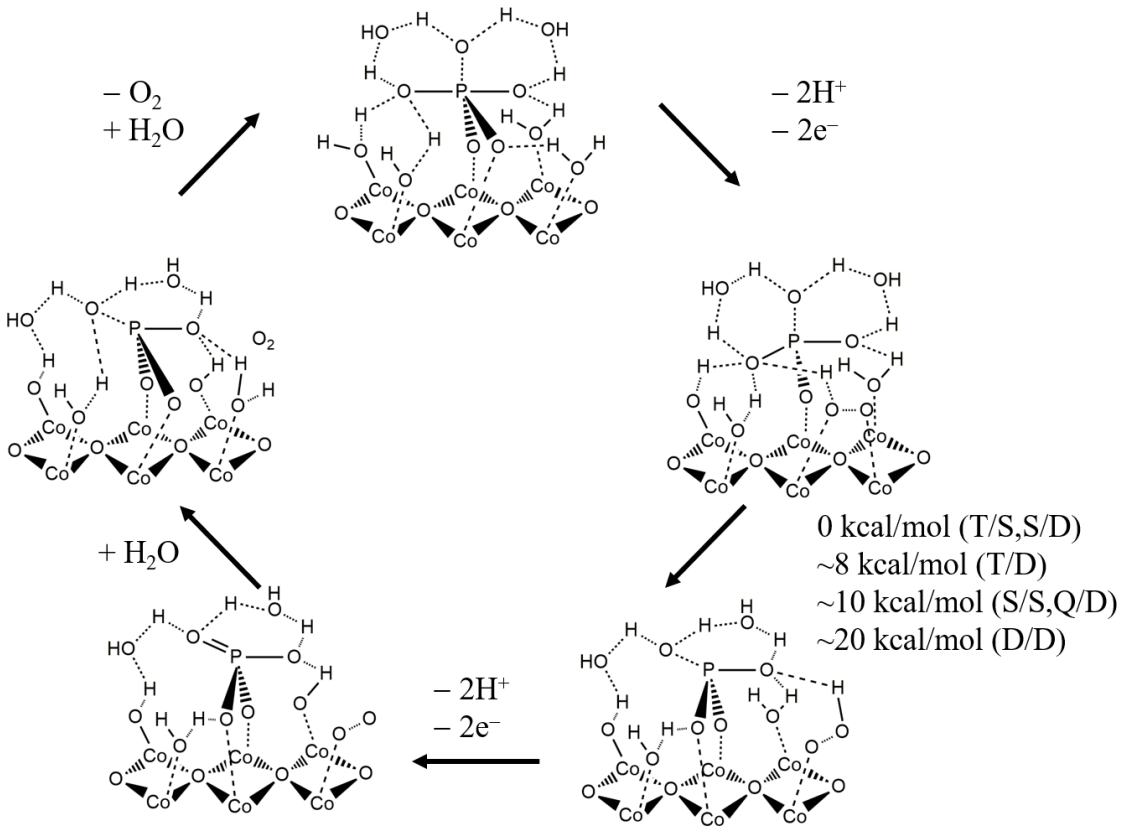

FIG. 9: Schematic of the water-oxidation reaction mechanism of the hydrated CoPi surface. The notation "S_1/S_2" indicates the spin states of the entire hydrated CoPi surface (S_1) and only the cobalt-oxide surface (S_2), e.g., "T/S" indicates the triplet state of the entire hydrated CoPi surface with the singlet state of the cobalt-oxide surface.

are presented for the triplet state of the doublet-state cobalt-oxide surface presented in Fig. S3, the singlet state of the singlet-state cobalt-oxide surface presented in Fig. S4, and the triplet state of the singlet-state cobalt-oxide surface presented in Fig. S5. This material is available free of charge via the Internet at xxxx.

FIGURE CAPTIONS

Fig. 1.

Calculated cluster models of the cobalt-oxide surface for the singlet and doublet electronic states from the surface and bottom sides. The difference between the models of the singlet and doublet states, which is the $Co(OH)_2$ fragment, are indicated by green dotted circles.

Fig. 2.

Reactant structures of the hydrated CoPi surface cluster model: the left-hand-side figure presents the schematic of the calculated surface cluster model and the right-hand-side figure presents the optimum geometry of the cluster model for the use of the singlet-state cobalt-oxide surface model. As shown in the surface structure model, for the model, one hydrogen atom is removed from one adsorbing water molecule of the singlet-state surface cluster model: the H-removed water molecules are indicated by (OH)" in red beside the corresponding water molecules.

Fig. 3.

Calculated vibrational spectrum of hydrated CoPi cluster model for the optimized reactant structure using the doublet-state cobalt-oxide surface in the singlet state. The curve at the top is the experimental FTIR spectrum of CoPi surface, which is excerpted from Ref.[40] for comparison. The main vibrational spectral band assignment is also shown.

Fig. 4.

Potential energy curves of hydrated CoPi cluster model using the doublet-state cobalt-oxide surface cluster model in the (a) singlet and (b) triplet electronic states for the extension of the distance between an O atom of the OOH group and the Co atom of its adsorption site. The potential energy is set as zero for the optimum hydrated CoPi structure before extending the O–Co distance. The optimum structures of the CoPi model before and after extending the O–Co distances are indicated by Min1 and Min2, respectively. In these optimum structures, the extended O–Co distances are indicated by orange arrows, and the formed O–O bonds are indicated by green dotted circles.

Fig. 5.

Potential energy curves of the hydrated CoPi cluster model using the doublet-state cobalt-oxide surface cluster model in the (a) doublet and (b) quartet electronic states for the extension of the distance between an O atom of the OOH group and the Co atom of its adsorption site. The potential energy is set as zero for the optimum hydrated CoPi structure before extending the O–Co distance. The optimum structures of the CoPi model before and after extending the O–Co distances are indicated by Min1 and Min2, respectively. In these optimum structures, the extended O–Co distances are indicated by orange arrows, and the formed O–O bonds are indicated by green dotted circles.

Fig. 6.

Potential energy curves of the hydrated CoPi cluster model using the singlet-state cobalt-oxide surface cluster model in the singlet and triplet electronic states for the extension of the distance between an O atom of the OOH group and the Co atom of its adsorption site. The potential energy is set as zero for the optimum hydrated CoPi structure before extending the O–Co distance. The optimum structures of the CoPi model before and after extending the O–Co distances are indicated by Min1 and Min2, respectively. In these optimum structures, the extended O–Co distances are indicated by orange arrows, and the formed O–O bonds are indicated by green dotted circles.

Fig. 7.

Water-oxidation reaction mechanism of the hydrated CoPi surface in the singlet state for the doublet-state cobalt-oxide surface. Formed O–O bonds are indicated by green circles.

Fig. 8.

The HOMO image of the reactant in the singlet state and the HOMO and lower SOMO images of Min2 in the singlet and triplet states, respectively, of the hydrated CoPi surface model, from which two electrons are released in the processes from reactant to Min1 and from Min2 to Min3 in the water-oxidation reaction mechanism (Fig. 7).

Fig. 9.

Schematic of the water-oxidation reaction mechanism of the hydrated CoPi surface. The notation "S_1/S_2" indicates the spin states of the entire hydrated CoPi surface (S_1) and only cobalt-oxide surface (S_2); "T/S" indicates the triplet state of the entire hydrated CoPi surface with the singlet state of the cobalt-oxide surface.

---

* Electronic address: tsuneda@phoenix.kobe-u.ac.jp

[1] Kanan, M. W.; Nocera, D. G. *Science* **2008**, *321*, 1072–1075.

[2] Kudo, A.; Miseki, Y. *Chem. Soc. Rev.* **2009**, *38*, 253–278.

[3] Maeda, K.; Domen, K. *J. Phys. Chem. Lett.* **2010**, *1*, 2655–2661.

[4] Jeon, T. H.; Choi, W.; Park, H. *Phys. Chem. Chem. Phys.* **2011**, *13*, 21392–21401.

[5] Surendranath, Y.; Kanan, M. W.; Nocera, D. G. *J. Am. Chem. Soc.* **2010**, *132*, 16501–16509.

[6] Lutterman, D. A.; Surendranath, Y.; Nocera, D. G. *J. Am. Chem. Soc.* **2009**, *131*, 3836–3839.

[7] McAlpin, J. G.; Surendranath, Y.; Dinca, M.; Stich, T. A.; Stoian, S. A.; Casey, W. H.; Nocera, D. G.; Britt, R. D. *J. Am. Chem. Soc.* **2010**, *132*, 6882–6883.

[8] Barroso, M.; Cowan, A. J.; Pendlebury, S. R.; Grätzel, M.; Klug, D. R.; Durrant, J. R. *J. Am. Chem. Soc.* **2011**, *133*, 14868–14871.

[9] Zhang, M.; de Respinis, M.; Frei, H. *Nature Chem.* **2014**, *6*, 362–367.

[10] Chen, J.; Selloni, A. *J. Phys. Chem. Lett.* **2012**, *3*, 2808–2814.

[11] Pham, H. H.; Cheng, M.-J.; Frei, H.; Wang, L.-W. *ACS Catal.* **2016**, *6*, 5610–5617.

[12] Wang, L.-P.; van Voorhis, T. *J. Phys. Chem. Lett.* **2011**, *2*, 2200–2204.

[13] Risch, M.; Khare, V.; Zaharieva, I.; Gerencser, Z. L.; Chernev, P.; Dau, H. *J. Am. Chem. Soc.* **2009**, *131*, 6936–6937.

[14] Kanan, M. W.; Yano, J.; Surendranath, Y.; Dinca, M.; Yachandra, V. K.; Nocera, D. G. *J. Am. Chem. Soc.* **2010**, *132*, 13692–13701.

[15] Tsuneda, T.; Hirao, K. *WIREs Comput. Mol. Sci.* **2014**, *4*, 375–390.

[16] Iikura, H.; Tsuneda, T.; Yanai, T.; Hirao, K. *J. Chem. Phys.* **2001**, *115*, 3540–3544.

[17] Tsuneda, T. *Density Functional Theory in Quantum Chemistry*; Springer: Tokyo, 2014.

[18] Tsuneda, T. *Int. J. Quantum Chem.* **2015**, *115*, 270–282.

[19] Tsuneda, T.; Song, J.-W.; Suzuki, S.; Hirao, K. *J. Chem. Phys.* **2010**, *133*, 174101(1–9).

[20] Nakata, A.; Tsuneda, T. *J. Chem. Phys.* **2013**, *139*, 064102(1–10).

[21] Nakatsuka, Y.; Tsuneda, T.; Sato, T.; Hirao, K. *J. Chem. Theor. Comput.* **2011**, *7*, 2233–2239.

[22] Suzuki, S.; Tsuneda, T.; Hirao, K. *J. Chem. Phys.* **2012**, *136*, 024706(1–6).

[23] Singh, R. K.; Tsuneda, T.; Miyatake, K.; Watanabe, M. *Chem. Phys. Lett.* **2014**, *608*, 11–16.

[24] Tsuneda, T.; Taketsugu, T. *Phys. Chem. Chem. Phys.* **2018**, *20*, 24992–24999.

[25] Tsuneda, T.; Tateyama, Y. *Phys. Chem. Chem. Phys.* **2019**, *21*, 22990–22998.

[26] Farrow, C. L.; Bediako, D. K.; Surendranath, Y.; Nocera, D. G.; Billinge, S. J. L. *J. Am. Chem. Soc.* **2013**, *135*, 6403–6406.

[27] Kohn, W.; Sham, L. J. *Phys. Rev. A* **1965**, *140*, 1133–1138.

[28] Becke, A. D. *Phys. Rev. A* **1988**, *38*, 3098–3100.

[29] Lee, C.; Yang, W.; Parr, R. G. *Phys. Rev. B* **1988**, *37*, 785–789.

[30] Tawada, Y.; Tsuneda, T.; Yanagisawa, S.; Yanai, T.; Hirao, K. *J. Chem. Phys.* **2004**, *120*, 8425–8433.

[31] Song, J.-W.; Hirosawa, T.; Tsuneda, T.; Hirao, K. *J. Chem. Phys.* **2007**, *126*, 154105.

[32] Peccati, F.; Laplaza, R.; Contreras-Garcia, J. *J. Phys. Chem. C* **2019**, *123*, 4767–4772.

[33] Janesko, B. G. *J. Phys. Chem. C* **2019**, *123*, 15062–15070.

[34] Gao, M.; Wang, B.; Tsuneda, T.; Lyalin, A.; Taketsugu, T. *J. Phys. Chem. C* **2021**, *125*, 19219–19228.

[35] Dunning Jr., T. H. *J. Chem. Phys.* **1989**, *90*, 1007–1023.

[36] Kendall, R. A.; Dunning, J. T. H.; Harrison, R. J. *J. Chem. Phys.* **1992**, *96*, 6796–6806.

[37] Hay, P. J.; Wadt, W. R. *J. Chem. Phys.* **1985**, *82*, 299–310.

[38] Tomasi, J.; Mennucci, B.; Cammi, R. *Chem. Rev.* **2005**, *105*, 2999–3093.

[39] Frisch, M. J. et al. Gaussian09 Revision D.01. 2009; Gaussian Inc. Wallingford CT.

[40] Hernandez-Contrerasa, X.-A.; Zumeta-Dubea, I.; Gattornoc, G. R.; Castrod, N. C.; Espinolae, J. L. C.; Reguera, E. *Appl. Catal. B: Environ.* **2021**, *282*, 119549(1–13).

[41] Tsuneda, T.; Miyake, J.; Miyatake, K. *ACS Omega* **2018**, *3*, 259–265.